International Journal of Nanomedicine Dovepress

Open Access Full Text Article ORIGINAL RESEARCH

Ultrasmall Antioxidant Copper Nanozyme to Enhance Stem Cell Microenvironment for Promoting Diabetic Wound Healing

Biao Hou[1,*], Chengyuan Li[2,*], Fen Yang[3,*], Wanjun Deng[1], Chao Hu[1], Changxiong Liu[1], Yanming Chen[1], Xiangjun Xiao[1], Xiongjie Huang[1], Jun Deng[1,4], Songlin Xie[1]

[1]Department of Hand and Foot Microsurgery, The Affiliated Nanhua Hospital, Hengyang Medical College, University of South China, Hengyang, Hunan, People's Republic of China; [2]Department of Pathology, School of Basic Medicine, Central South University, Changsha, Hunan, People's Republic of China; [3]Department of Infectious Diseases, The Affiliated Nanhua Hospital, Hengyang Medical College, University of South China, Hengyang, Hunan, People's Republic of China; [4]Institute of Burn Research, Southwest Hospital, State Key Laboratory of Trauma, Burn and Combined Injury, Chongqing Key Laboratory for Disease Proteomics, Army Medical University, Chongqing, People's Republic of China

*These authors contributed equally to this work

Correspondence: Songlin Xie; Jun Deng, Email xiesonglin0929@163.com; djun.123@163.com

Purpose: Stem cell therapy is a promising approach for treating chronic diabetic wounds. However, its effectiveness is significantly limited by the high oxidative stress environment and persistent inflammation induced by diabetes. Strategies to overcome these challenges are essential to enhance the therapeutic potential of stem cell therapy.

Methods: $Cu_{5.4}O$ ultrasmall nanoparticles ($Cu_{5.4}O$-USNPs), known for their excellent reactive oxygen species (ROS) scavenging properties, were utilized to protect adipose-derived stem cells (ADSCs) from oxidative stress injury. In vitro experiments were conducted to evaluate the viability, paracrine activity, and anti-inflammatory capabilities of ADSCs loaded with $Cu_{5.4}O$-USNPs under oxidative stress conditions. In vivo experiments in diabetic mice were performed to assess the therapeutic effects of $Cu_{5.4}O$-USNP-loaded ADSCs on wound healing, including their impact on inflammation, collagen synthesis, angiogenesis, and wound closure.

Results: ADSCs treated with $Cu_{5.4}O$-USNPs showed significantly enhanced viability, paracrine activity, and anti-inflammatory properties under oxidative stress conditions in vitro. In diabetic mice, $Cu_{5.4}O$-USNP-loaded ADSCs reduced inflammatory responses in wound tissues, promoted collagen synthesis and angiogenesis, and accelerated diabetic wound healing. These findings suggest that $Cu_{5.4}O$-USNPs effectively mitigate the adverse effects of oxidative stress and inflammation, enhancing the therapeutic efficacy of ADSCs.

Conclusion: This study presents a simple and effective approach to improve the therapeutic potential of stem cell therapy for diabetic wounds. By incorporating $Cu_{5.4}O$-USNPs, the antioxidative and anti-inflammatory capabilities of ADSCs are significantly enhanced, offering a promising strategy for ROS-related tissue repair and chronic wound healing.

Keywords: stem cell therapy, $Cu_{5.4}O$-USNPs, ADSCs, inflammatory environment

Introduction

The continuous development of stem cell therapy has brought hope for many incurable diseases. Stem cells, undifferentiated cells with the potential for self-renewal and differentiation into various cell types, exhibit remarkable proliferation capacity.[1] Among them, mesenchymal stem cells (MSCs) derived from sources such as bone marrow, adipose tissue, and umbilical cord offer advantages including diverse sourcing, straightforward preparation, safety, efficacy, and relatively low immunogenicity. Consequently, MSC therapy has achieved significant success in treating skin wounds,[2] neurological disorders,[3] cardiovascular conditions,[4] endocrine diseases,[5] and facilitating organ transplants.[6] MSC has demonstrated remarkable potential in tissue repair, particularly in accelerating wound healing. MSCs can home to damaged areas, enhancing repair efficiency.[7] Furthermore, their multi-directional differentiation potential allows them

Received: 19 July 2024
Accepted: 13 December 2024
Published: 19 December 2024

to differentiate into various tissue cells in vitro.[8] Through the production of cytokines, growth factors, and extracellular vesicles, MSCs' paracrine function creates a favorable repair environment, regulates immune reactions, and promotes tissue repair.[9,10] However, significant challenges remain for this emerging medical technology, including administration methods,[11] constraints on ex vivo expansion, immune rejection,[12] and unsuitable transplantation microenvironments.[13]

At injury sites, oxidative stress frequently occurs due to adverse reactions triggered by free radicals, resulting from an imbalance between oxidative and antioxidative processes within the body. Elevated oxidative levels escalate the accumulation of oxidative damage byproducts, precipitating disease onset and aging. Reactive oxygen species (ROS), considered the main cause of oxidative stress, include molecules such as $\cdot O^{2-}$, H_2O_2, and $\cdot OH$.[14,15] Under normal physiological conditions, their concentration is low and in dynamic equilibrium. At these levels, ROS act as important signaling mediators, participating in the regulation of cell fate and various physiological functions.[16,17] The dynamic balance of intracellular ROS is regulated by various cellular processes that generate and remove ROS. Excessive ROS production negatively affects cell structures such as membranes, lipids, proteins, lipoproteins, and DNA,[18,19] leading to the development of diseases such as cancer,[20,21] cardiovascular diseases,[22,23] nervous system disorders,[24–27] and chronic wounds.[28,29]

In chronic wounds, local tissue remains inflamed and ischemic due to prolonged infection and vascular degeneration, leading to abnormal cellular metabolism and excessive ROS production. Sustained oxidative stress damages various skin cells and perpetuates chronic inflammation, while also inhibiting the cell's own defense mechanisms. These factors ultimately delay tissue repair, causing wounds to persist without healing. Numerous studies have reported the application of stem cells, particularly MSCs, in treating chronic wounds. Numerous studies have documented the advancements in utilizing adipose-derived stem cells (ADSCs) for the treatment of chronic wounds.[30–32] For example, fibrin-induced ADSCs have been shown to facilitate capillary-like structure formation in vitro, contributing to chronic wound healing. Additionally, ADSCs have demonstrated the ability to enhance tissue regeneration in diabetic wounds, highlighting their therapeutic potential in wound repair.[33,34] However, MSCs exhibit low antioxidant activity and are sensitive to oxidative stress.[35–37] Following transplantation and homing to the injured site, oxidative stress inhibits MSC proliferation and induces apoptosis, significantly reducing their activity. The surviving MSCs fail to produce sufficient cytokines and growth factors, thus lacking therapeutic efficacy. Hence, exploring new methods to enhance MSC activity and function in oxidative stress environments is of great significance.[38]

Recent advancements in nanotechnology and enzymology have led to the development of various nanomaterials that mimic enzymatic activities and scavenge ROS.[39] For instance, MnO_2 nanoparticle-hydrogel composites can effectively modulate the ROS microenvironment by catalyzing the decomposition of H_2O_2 into H_2O and O_2. This process significantly enhances the efficacy of stem cells in treating spinal cord injuries.[40] Similarly, Fullerenol nanoparticles can interact with ROS at the electron-deficient sites on their surface, facilitating the elimination of ROS through electron transfer. This mechanism significantly enhances the survival rate of stem cells within alginate hydrogels in ROS-rich environments.[41] Gold nanoparticles linked with 2,2,6,6-tetramethylpiperidine-N-oxyl effectively lower ROS levels in stem cell cultures.[42] Furthermore, bovine serum albumin/heparin nanoparticles remove ROS from tendon stem cell environments, preventing calcification,[43] while polydopamine nanoparticles enhance neuroprotection in stem cells against hypoxic damage.[44] Ursodeoxycholic acid polymer-based nanoparticles also augment the antioxidant and anti-inflammatory properties of stem cells, facilitating bone regeneration.[45] These findings underscore the critical role of ROS-scavenging nanoparticles in stem cell therapy. Incorporating such nanomaterials in the treatment of diabetic wounds with MSCs could improve their survival and reparative capabilities at the injury site, thereby delivering expected therapeutic outcomes.

We previously reported on ultrasmall copper-based nanoparticles—$Cu_{5.4}O$ ultrasmall nanoparticles ($Cu_{5.4}O$-USNPs)—that exhibit enzyme-mimicking capabilities and a broad spectrum of reactive oxygen species (ROS) scavenging activities for the treatment of ROS-related diseases.[46] Compared to other nanozymes, $Cu_{5.4}O$-USNPs offer several unique advantages: (1) an ultrasmall particle size; (2) excellent biocompatibility with negligible toxicity and a high renal clearance rate; (3) straightforward synthesis procedures that facilitate large-scale production and easy reproducibility; (4) the ability to simultaneously mimic catalase, superoxide dismutase, and glutathione peroxidase, showcasing outstanding ROS scavenging efficiency; and (5) broad-spectrum ROS scavenging capability' (6) Yang et al investigated

and discussed the potential of these copper nanoparticles in promoting wound healing.[47] Therefore, $Cu_{5.4}O$-USNPs serve as an ideal ROS scavenger, indicating their potential as a promising nanomaterial for enhancing the survival and functionality of stem cells post-transplantation. In this study, we introduced them into adipose-derived stem cells (ADSCs), leveraging their enzyme-mimicking properties and broad-spectrum ROS scavenging capacity, along with good biocompatibility. The $Cu_{5.4}O$-USNPs enhanced cellular activity, paracrine function, and anti-inflammatory responses of ADSCs under oxidative stress by effectively scavenging ROS. Additionally, in a diabetic mouse wound model, ADSCs loaded with $Cu_{5.4}O$-USNPs demonstrated improved wound healing efficacy (Scheme 1). This research is significant for enhancing the therapeutic potential of ADSCs and offers a novel approach to the clinical treatment of chronic wounds.

Materials and Methods

Materials

Copper chloride powder ($CuCl_2$), L-ascorbic acid (AA), and sodium hydroxide, all purchased from J&K Scientific (Beijing, China), were utilized in the synthesis of $Cu_{5.4}O$ ultrasmall nanoparticles ($Cu_{5.4}O$-USNPs). Phosphate-buffered saline (PBS) and RAW264.7 cell lines were sourced from Pricella (Wuhan, China), while the superoxide anion assay kit was acquired from Jiancheng Bioengineering Institute (Nanjing, China). The CCK-8 cell proliferation toxicity assay kit and DCFH-DA reactive oxygen species assay kit were procured from Applygen (Beijing, China). ELISA kits for mouse vascular endothelial growth factor (VEGF), interleukin-10 (IL-10), and tumor necrosis factor-alpha (TNF-α) were obtained from Mlbio (Shanghai, China). Lipopolysaccharide (LPS, L2880) was sourced from Sigma (USA). Streptozotocin (STZ), sodium citrate buffer, hematoxylin-eosin (HE) staining kit, and Masson's trichrome staining kit were provided by Solarbio (Beijing, China). Xylene, anhydrous ethanol, and methanol were procured from Macklin

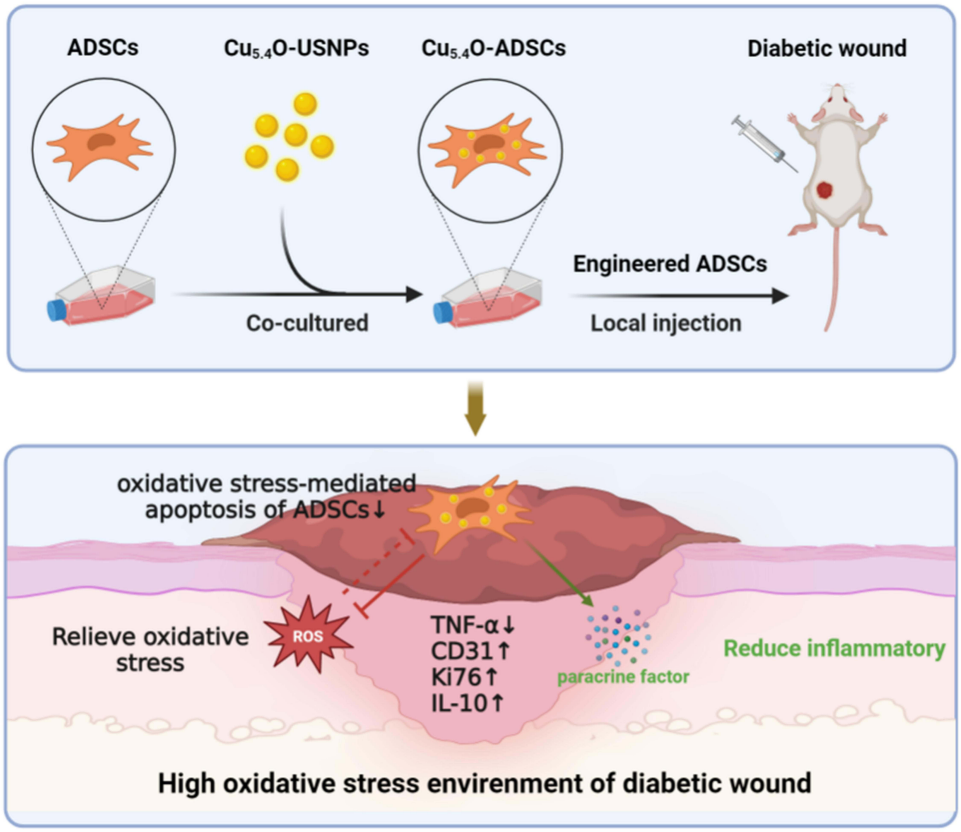

Scheme 1 Cu5.4O-USNPs were integrated into ADSCs to enhance their survival, paracrine signaling, and anti inflammatory properties under oxidative stress conditions, resulting in significant therapeutic benefits.

(Shanghai, China). All chemicals and reagents were of analytical grade and did not require further purification. Ultrapure water from a Milli-Q water purification system (Merck Millipore, Germany) was used throughout the experiments.

Preparation and Characterization of $Cu_{5.4}O$-USNPs

The synthesis of $Cu_{5.4}O$-USNPs followed established methodologies.[40] Initially, 10 mm $CuCl_2{\cdot}2H_2O$ powder was dissolved in 50 mL of ultrapure water and stirred at 80°C for 10 minutes. Subsequently, 100 mm L-ascorbic acid aqueous solution (50 mL) was added dropwise while stirring continuously to ensure thorough mixing. The pH of the solution was adjusted to 8.0–9.0 by adding 1 M sodium hydroxide solution. The mixture was stirred and maintained at 80°C for 14–16 hours. Post-reaction, the solution underwent centrifugation at 6577g for 15 minutes to eliminate larger impurities. The supernatant was dialyzed for two days to remove small molecules, and the $Cu_{5.4}O$-USNPs were concentrated and purified by further centrifugation. Transmission electron microscopy was employed to examine the $Cu_{5.4}O$-USNPs samples.

Various concentrations of $Cu_{5.4}O$-USNPs (0, 50, 100, 150, 200 ng/mL) were tested. Oxidative stress conditions were simulated using 2 mm H_2O_2, with samples incubated at 37°C for 2 hours. A 0.1 mL aliquot of each test sample was added to a detection tube, and the optical density (OD) value was measured using a microplate reader.

Cell Culture

Mouse adipose stem cell lines were acquired from ICell Bioscience Inc (Shanghai, China). ADSCs were cultured in flasks containing 5 mL of complete medium, which consisted of 90% Dulbecco's Modified Eagle Medium (DMEM), 10% fetal bovine serum (FBS), and 1% penicillin-streptomycin (PS). The cultivation process took place in an incubator set at 37°C with an atmosphere of 5% CO_2.

Cell Viability and Functional Assessment of ADSCs Loaded with $Cu_{5.4}O$-USNPs

Approximately 10,000 ADSCs were cultured per well in a 96-well plate for 24 hours. Subsequently, the wells were treated with 100 μL of medium containing $Cu_{5.4}O$-USNPs at concentrations ranging from 0 to 7 μg/mL and incubated for an additional 24 hours. This was followed by the addition of 100 μL of serum-free medium and 10 μL of CCK-8 reagent. After 1 hour of incubation in the dark, OD values were measured using a microplate reader (BioTek, USA).

To induce an oxidative stress environment, H_2O_2 at concentrations of 0 to 200 μM was added to the wells, and cell viability was assessed using CCK-8 after another 24 hours of incubation. A scratch assay was performed by seeding ADSCs in a 6-well plate and creating a vertical scratch across the cell monolayer using a pipette tip. Cells were washed three times with PBS to remove any detached cells, and migration was documented at 0, 24, and 48 hours. For ROS detection, ADSCs in a 6-well plate were incubated with 2 mL of 10 μM DCFH-DA in serum-free medium for 30 minutes, and fluorescence intensities were visualized using a fluorescence microscope.

After 24 hours of seeding ADSCs in a 6-well plate, cells were centrifuged at 1000 rpm for 5 minutes. The pellet was resuspended in 10 μM DCFH-DA and incubated in the dark for 30 minutes, followed by centrifugation at 1000g for 20 minutes. Cells were washed twice with PBS and then analyzed for intracellular ROS using flow cytometry (BD, USA). ELISA kits were employed to quantify VEGF secretion and anti-inflammatory responses in ADSCs and $Cu_{5.4}$ O-ADSCs under both non-oxidative and oxidative conditions at 24, 48, and 72 hours, respectively.

Construction of Diabetic Mouse Wound Model

Five-week-old male Kunming (KM) mice, weighing 35–45g, were selected for the study. All experimental animals were specific pathogen-free grade (SPF-grade) and were purchased from Hunan Silaikejingda Experimental Animal Co., Ltd. The mice underwent a one-week acclimatization period before modeling. After a 12-hour fasting period, the mice received intraperitoneal injections of STZ solution at a dose of 50 mg/kg for five consecutive days to induce diabetes. Mice were evaluated and considered diabetic when fasting blood glucose levels consistently exceeded 16.7 mmol L^{-1} for 3 weeks after the initial STZ administration, as in previous reports.[46] If the blood glucose level did not exceed 16.7 mmol/L, additional STZ injections were administered, and blood glucose was monitored again.

Assessment of Wound Healing Effectiveness

Following anesthesia with isoflurane (Abbott, USA), the back hair of each mouse was shaved, and the exposed skin was disinfected. Symmetric circular full-thickness skin defects, 10 mm in diameter, were then created on both sides of the midline of the mouse's back. Post-surgery, all mice were housed individually to prevent mutual biting from affecting the experimental results. The diabetic mice were randomly assigned into three groups, each consisting of eight mice (n=8). Localized injections at the wound margins were administered as follows: (A) 100 μL PBS (DM group); (B) 100 μL PBS containing 5×10^5 ADSCs (ADSC group); (C) 100 μL PBS containing 5×10^5 $Cu_{5.4}O$-ADSCs ($Cu_{5.4}O$-ADSC group). Wound healing in each group was documented on days 0, 3, 5, 7, and 14 post-surgery.

On the 7th and 14th days post-surgery, complete skin tissues, including approximately 5 mm around the wound edge, were excised and embedded in paraffin. Sections were stained with H&E and Masson's trichrome. Automated slide scanners (Zeiss, Germany) scanned the sections, and ImageJ software was used to analyze histological changes and collagen content in each group.

Immunohistochemistry Analysis

To evaluate cell proliferation, angiogenesis, and inflammation in wound tissues, immunohistochemical staining for Ki67, CD31, TNF-α, and IL-10 (all from Abcam, USA) was performed on tissue sections. The experiment followed the provided instructions. Sections were incubated overnight at 4°C with primary antibodies against Ki67, CD31, TNF-α, and IL-10, followed by a 1-hour incubation with secondary antibodies (Abcam, USA). Automated slide scanners were utilized for scanning, and ImageJ software was used for analyzing and quantifying positive cells in each group.

Statistical Analysis

Results are presented as mean ± standard deviation (SD). Intergroup differences were assessed using one-way analysis of variance (ANOVA), with statistical significance set at $P < 0.05$. All statistical analyses and graphical representations were performed using GraphPad Prism 8 software.

Results

Characterizations of $Cu_{5.4}O$-ADSCs

TEM results revealed that $Cu_{5.4}O$-USNPs appeared as uniformly distributed spherical particles with diameters ranging from 3 to 6 nm, with an average diameter of 4.83 ± 1.55 nm (Figure 1A and B). An in vitro oxidative stress environment was simulated using 2 mm H_2O_2 to evaluate the ROS scavenging ability of $Cu_{5.4}O$-USNPs. Results indicated that the efficiency of H_2O_2 removal increased with the concentration of $Cu_{5.4}O$-USNPs, demonstrating a concentration-dependent ROS scavenging ability (Figure 1C). At a concentration of 200 ng/mL, the H_2O_2 removal efficiency exceeded 80%. This finding aligns with previous studies, showing that $Cu_{5.4}O$-USNPs exhibit high scavenging efficiency even at low concentrations.[46] ADSCs treated with varying concentrations of $Cu_{5.4}O$-USNPs for 24 hours showed that concentrations up to 1000 ng/mL exhibited virtually no cytotoxicity compared to the control group (Figures 1D–F), demonstrating the good biocompatibility of $Cu_{5.4}O$-USNPs.

$Cu_{5.4}O$-USNPs Enhance the Antioxidant Stress Capacity of ADSCs

H_2O_2 at various concentrations was used to stimulate the cells, with the IC_{50} value from cytotoxicity assays establishing the inducer concentration for an in vitro oxidative stress model. After stimulating ADSCs with H_2O_2 (50–200 μM) for 24 hours, a significant decrease in cell viability correlated with increasing H_2O_2 concentration (Figure 2A). The calculated average IC_{50} value from multiple experiments was approximately 98 μM.

To assess the antioxidant capacity of $Cu_{5.4}O$-USNP-loaded ADSCs, cells were treated with $Cu_{5.4}O$-USNPs at safe concentrations (0, 200, 400, 600, 800, 1000 ng/mL) before inducing oxidative stress. Results indicated a concentration-dependent increase in cell viability, approaching that of normal, untreated cells, which demonstrates the ROS scavenging ability of $Cu_{5.4}O$-USNPs. Even at 1000 ng/mL, ADSCs maintained high viability (Figure 2B). Intracellular ROS levels were measured in both ADSCs and $Cu_{5.4}O$-ADSCs under oxidative stress, with ROS levels in non-oxidative conditions

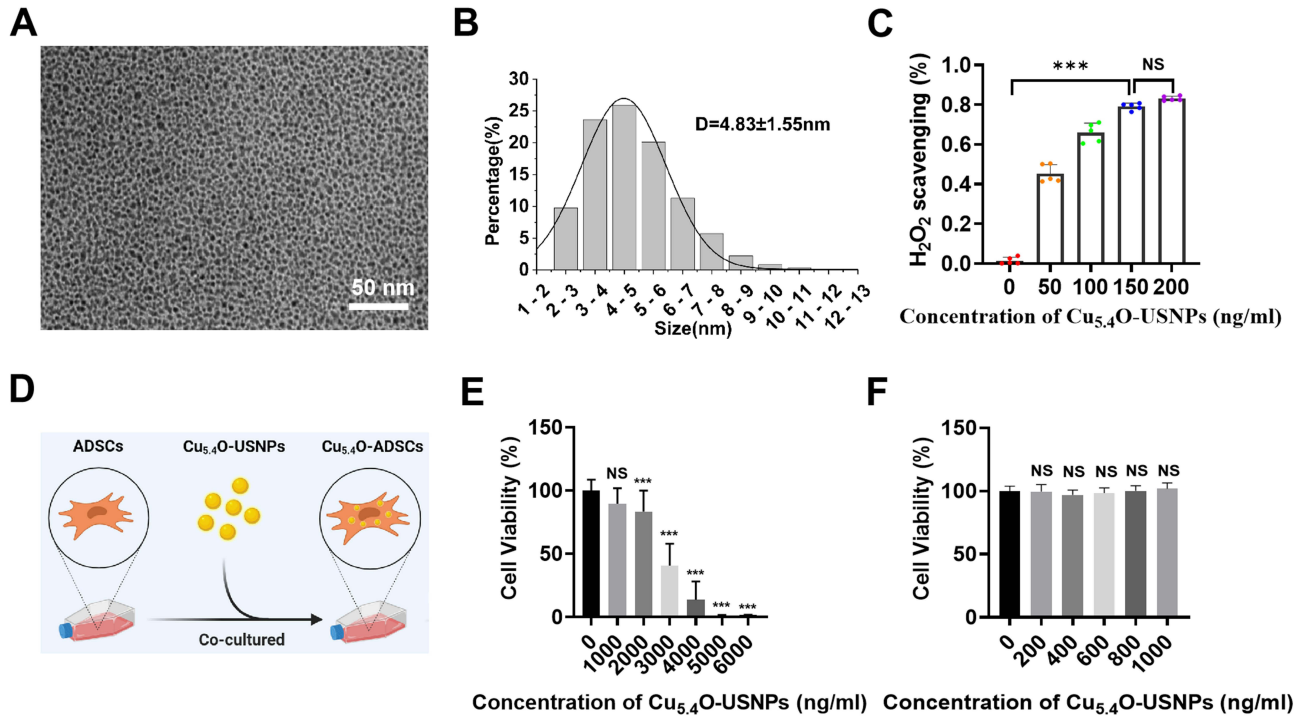

Figure 1 (**A**) TEM image of $Cu_{5.4}O$-USNPs. (**B**) Particle size distribution of $Cu_{5.4}O$-USNPs determined from TEM image analysis (n=300). (**C**) In vitro H_2O_2 scavenging efficiency of $Cu_{5.4}O$-USNPs (2 mm H_2O_2). (**D**) Cell viability of ADSCs loaded with different concentrations (0–7000 ng/mL) of $Cu_{5.4}O$-USNPs. (**E**) Cell viability of ADSCs loaded with different concentrations (0–6000 ng/mL) of $Cu_{5.4}O$-USNPs. (**F**) Cell viability of ADSCs loaded with different concentrations (0–1000 ng/mL) of $Cu_{5.4}O$-USNPs. ***P<0.001, NS P>0.05.

serving as the control. The fluorescence intensity of $Cu_{5.4}O$-ADSCs was similar to the control group, whereas the untreated ADSCs exhibited the highest fluorescence intensity (Figure 2C and D), indicating reduced intracellular ROS levels in $Cu_{5.4}O$-ADSCs. Flow cytometry confirmed these findings (Figure 2E and F), demonstrating that $Cu_{5.4}O$-USNPs enhance the antioxidant capacity of ADSCs under oxidative stress.

The scratch test revealed that $Cu_{5.4}O$-USNPs promote ADSC migration and proliferation in oxidative stress conditions (Figure 2G). At 24 hours, the $Cu_{5.4}O$-ADSCs group showed migration ability comparable to the control group (normal ADSCs in non-oxidative conditions), while the untreated ADSCs displayed reduced migration. By 48 hours, the scratch area was nearly closed in both the control and $Cu_{5.4}O$-ADSCs groups. Analysis of cell migration rates indicated that $Cu_{5.4}O$-ADSCs had higher migration rates than untreated ADSCs at both 24 and 48 hours (Figure 2H), with no statistical difference compared to the control group ($P > 0.05$).

$Cu_{5.4}O$-USNPs Enhance the Paracrine and Anti-Inflammatory Functions of ADSCs

An oxidative stress environment was simulated using a complete culture medium containing 100 μM H_2O_2. Subsequently, the VEGF secretion function of ADSCs and $Cu_{5.4}O$-ADSCs was assessed under both non-oxidative and oxidative stress conditions. Results indicated that in a normal environment, VEGF secretion levels in both ADSCs and $Cu_{5.4}O$-ADSCs gradually increased over time without significant differences between the groups at corresponding time points ($P > 0.05$) (Figure 3A). However, under oxidative stress, VEGF secretion significantly decreased in both groups, indicating that oxidative stress impairs the cells' paracrine function. Over time, VEGF secretion levels in both groups under oxidative stress gradually increased, but the levels in the ADSCs group remained consistently lower than those in the $Cu_{5.4}O$-ADSCs group at the same time points ($P < 0.01$) (Figure 3B). This suggests that oxidative stress inhibits the paracrine function of ADSCs, and loading $Cu_{5.4}O$-USNPs, with their ROS scavenging ability, reduces intracellular or environmental ROS, thereby mitigating the negative effects of oxidative stress and enhancing paracrine function. These results indicate that $Cu_{5.4}O$-USNPs improve the antioxidant capacity of cells under oxidative stress, thereby enhancing their suppressed paracrine function.

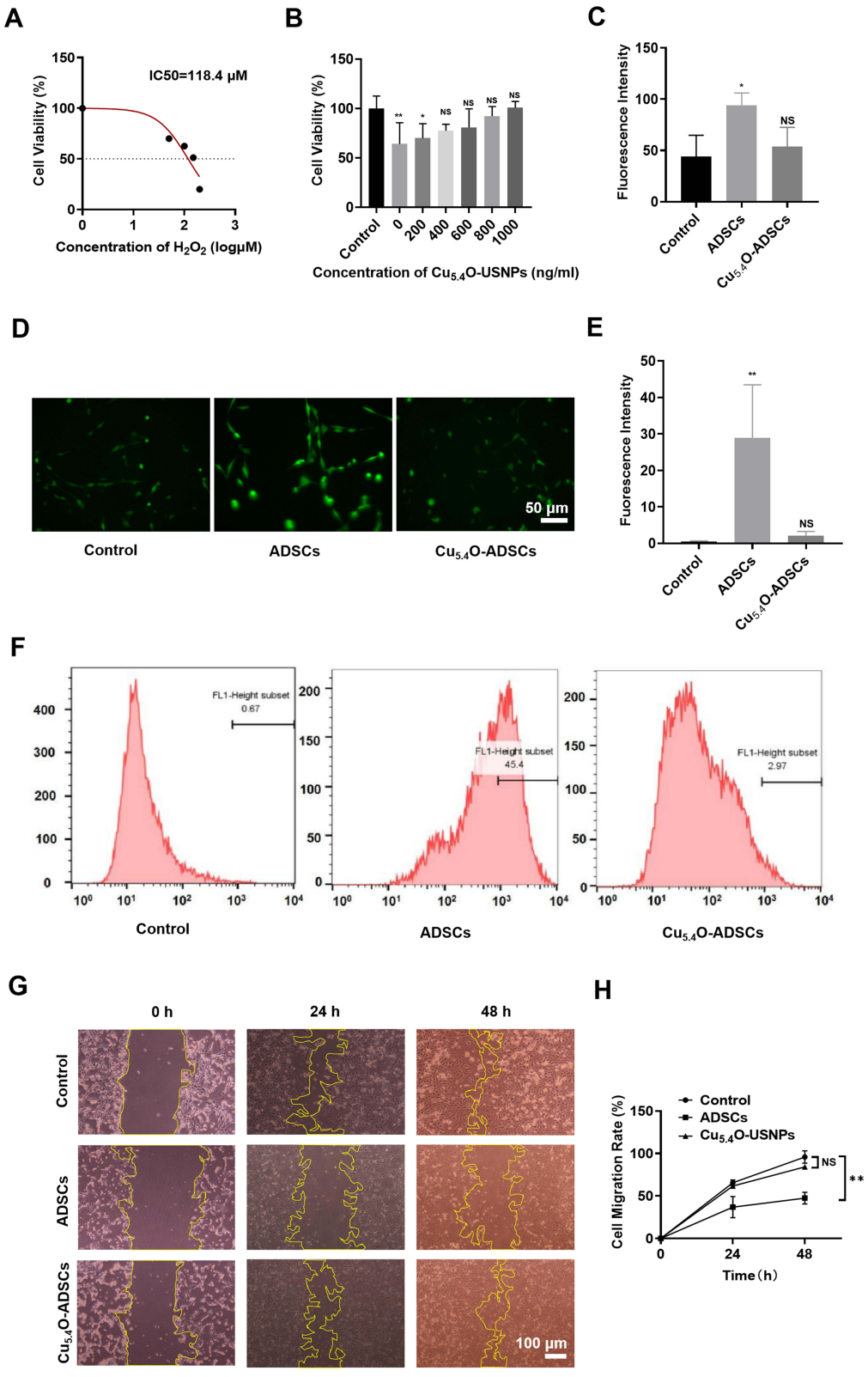

Figure 2 (**A**) Cell viability and IC_{50} of ADSCs after 24 hours of stimulation with 0–200 μM H_2O_2. (**B**) Cell viability of $Cu_{5.4}O$-ADSCs at different concentrations after 24 hours of stimulation with 100 μM H_2O_2. (**C** and **D**) Microscopic scratch images of different treatment groups at three time points: 0h, 24h, and 48h. (**E**) Representative images of different treatment groups after DCFH-DA staining under a fluorescence microscope. (**F**) Intracellular ROS content of different treatment groups obtained by flow cytometry. (**G**) Average fluorescence intensity of different groups under a fluorescence microscope. (**H**) Relative fluorescence intensity of different treatment groups obtained from flow cytometry results. *P<0.05,** P<0.01, NS P>0.05.

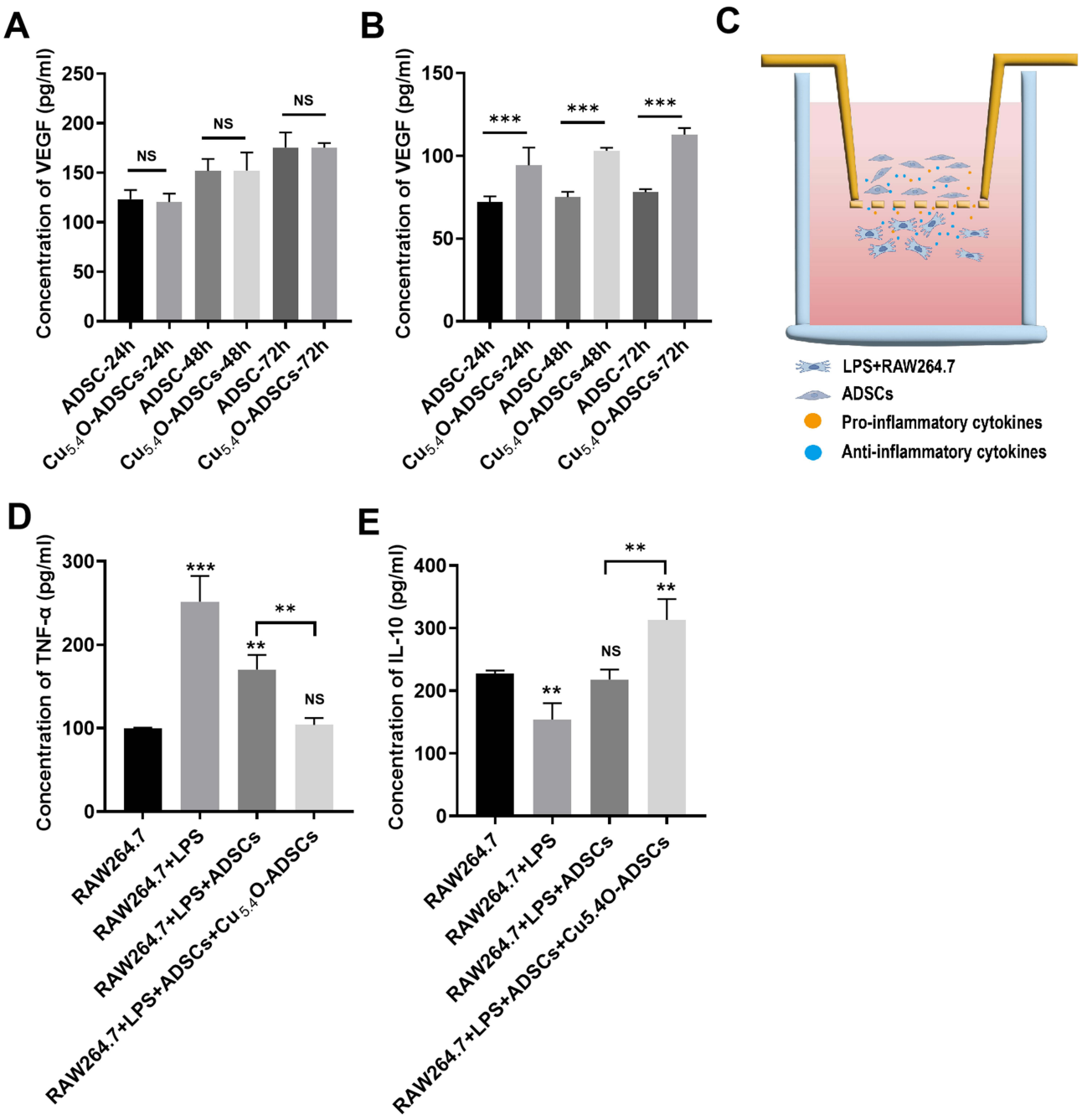

Figure 3 (**A**) VEGF secretion levels of ADSCs and $Cu_{5.4}O$-ADSCs at 24h, 48h, and 72h under normal conditions. (**B**) VEGF secretion levels of ADSCs and $Cu_{5.4}O$-ADSCs at 24h, 48h, and 72h under oxidative stress conditions. (**C**) Schematic diagram of the co-culture system of RAW264.7 and ADSCs. (**D**) TNF-α levels secreted by different treatment groups. (**E**) IL-10 levels secreted by different treatment groups. ** $P<0.01$,***$P<0.001$, NS $P>0.05$.

A co-culture system of ADSCs and RAW264.7 was subsequently established by seeding these cell types in the upper and lower chambers of a six-well plate equipped with a Transwell insert. In this system, a polycarbonate membrane with 0.4 μm pores separates the two cell types, preventing direct contact while allowing cytokines secreted by cells in both layers to pass through and influence each other's physiological state and functions. An in vitro inflammation model was constructed by seeding ADSCs in the upper chamber and RAW264.7 cells treated with 2 μg/mL LPS for 24 hours in the lower chamber.[48] (Figure 3C) This model simulates the inflammatory environment at injury sites where stem cells are transplanted, allowing the study of $Cu_{5.4}O$-USNPs' anti-inflammatory effects on ADSCs under inflammatory conditions. Results demonstrated that the RAW264.7 + LPS group exhibited higher levels of pro-inflammatory factors and lower levels of anti-inflammatory factors

compared to the RAW264.7 group alone, confirming the successful activation of RAW264.7 by LPS. Levels of pro-inflammatory factors secreted by the RAW264.7 + LPS + ADSCs group and RAW264.7 + LPS + $Cu_{5.4}O$-ADSCs group were lower than those in the RAW264.7 + LPS group, while anti-inflammatory factor levels were higher. Notably, the RAW264.7 + LPS + $Cu_{5.4}O$-ADSCs group showed a more significant reduction in pro-inflammatory factors and an increase in anti-inflammatory factors compared to the RAW264.7 + LPS + ADSCs group (Figure 3D and E). These findings suggest that $Cu_{5.4}O$-USNPs enhance the antioxidant capacity of cells in an inflammatory environment, thereby improving their suppressed anti-inflammatory capability.

$Cu_{5.4}O$-ADSCs Promoted Wound Healing in Diabetic Mice

To assess the therapeutic effects of $Cu_{5.4}O$-USNP-loaded ADSCs on diabetic mouse wounds, wound conditions were recorded at five time points: day 0, day 3, day 5, day 7, and day 14 post-surgery. On postoperative day 0, the wound areas were comparable across all groups (Figure 4A). By day 3, the $Cu_{5.4}O$-ADSCs group exhibited a significantly faster healing rate compared to the other groups ($P < 0.05$). Over time, wound healing rates increased for all groups, with the $Cu_{5.4}O$-ADSCs group consistently showing the highest rate. By day 14, wounds in the $Cu_{5.4}O$-ADSCs group were nearly completely healed (Figure 4A and B). These findings suggest that $Cu_{5.4}O$-USNPs enhance ADSCs' wound-healing capabilities in diabetic mice.

HE staining of wound specimens from each group on days 7 and 14 post-surgery revealed that on day 7, both the ADSCs and $Cu_{5.4}O$-ADSCs groups displayed visible dermal tissue growth towards the wound center, while the DM group did not show significant dermal tissue growth (Figure 5A). By day 14, the DM group had a large number of infiltrated inflammatory cells and a larger wound defect, whereas the $Cu_{5.4}O$-ADSCs group exhibited superior wound healing with fewer inflammatory cells, continuous dermal tissue, and a more mature tissue structure. These results indicate that $Cu_{5.4}O$-USNPs improve ADSCs' ability to promote dermal formation and reduce inflammation.

Masson trichrome staining on wound specimens from each group on days 7 and 14 post-surgery assessed collagen and muscle fiber growth. On day 7, the DM and ADSCs groups showed minimal collagen fiber deposition, while the $Cu_{5.4}O$-ADSCs group showed the most (Figure 5B and C). By day 14, collagen fiber content differences were more pronounced, with the $Cu_{5.4}O$-ADSCs group showing significantly more collagen fiber deposition, while the DM group showed the least. These findings suggest that $Cu_{5.4}O$-USNPs enhance ADSCs' ability to promote collagen synthesis.

Immunohistochemical staining for Ki67 was performed on wound tissues on postoperative day 14 to assess cell proliferation. Ki67, an antigen associated with cell proliferation, showed significantly lower positive rates in the DM group compared to the ADSCs group ($P < 0.01$), and lower in the ADSCs group than the $Cu_{5.4}O$-ADSCs group ($P < 0.01$) (Figure 6A). This suggests that loading $Cu_{5.4}O$-USNPs enhances the proliferative capacity of ADSCs.

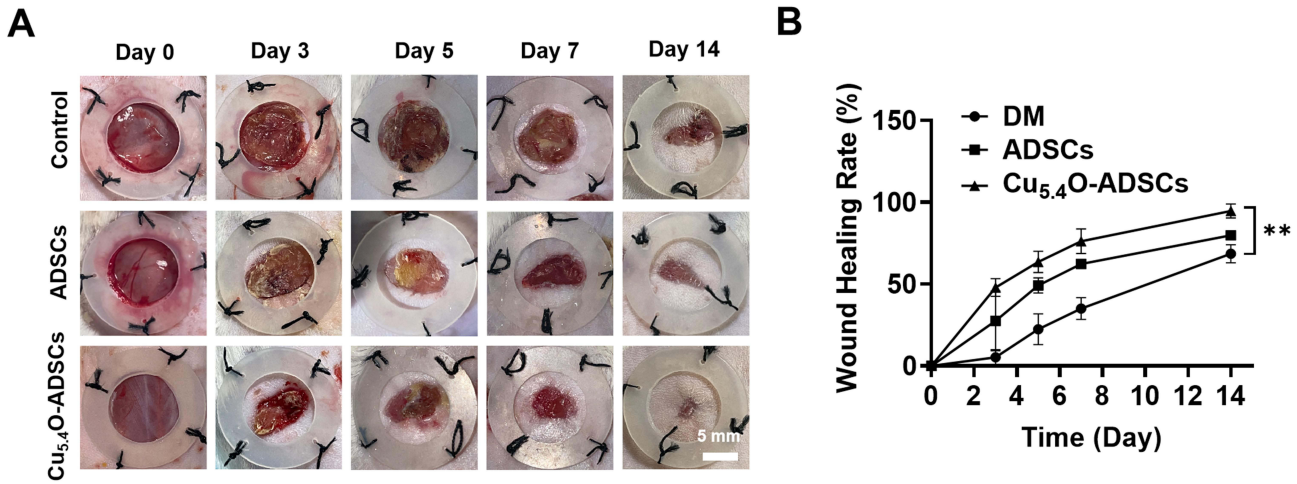

Figure 4 (**A**) Wound healing process and (**B**) wound closure rate of diabetic mice in different treatment groups. ** $P<0.01$.

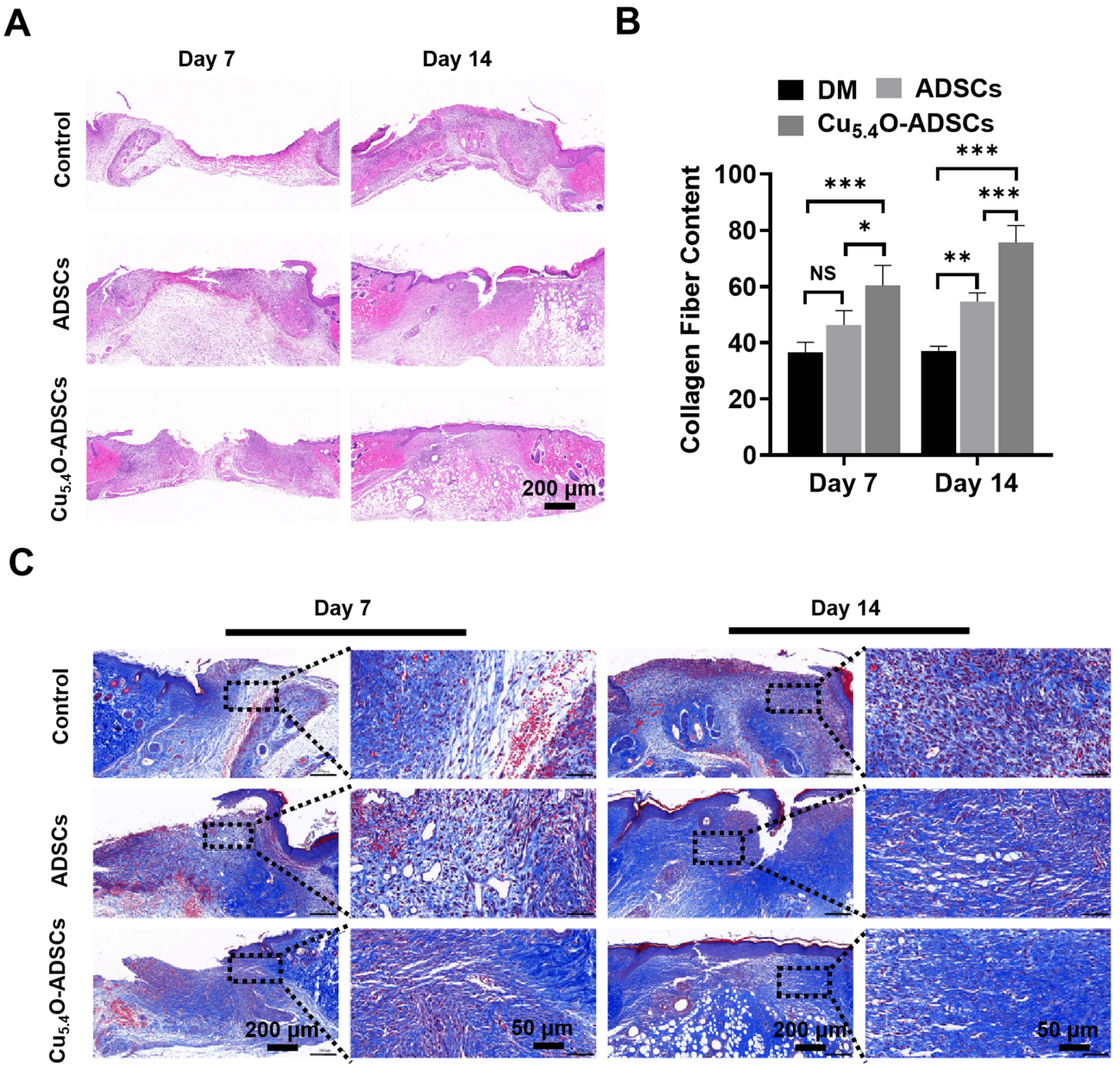

Figure 5 (**A**) Histological sections of wound sites stained with H&E on postoperative days 7 and 14 in different treatment groups of diabetic mice. (**B** and **C**) Histological sections of wound sites stained with Masson's trichrome on postoperative days 7 and 14 in different treatment groups of diabetic mice. Blue represents collagen fibers, and red represents muscle fibers. *P<0.05,** P<0.01,***P<0.001, NS P>0.05.

CD31 staining, which identifies endothelial cells and reflects blood vessel formation, revealed significantly lower positive rates in the DM group compared to the ADSCs group ($P < 0.001$), and a significant difference between the ADSCs group and the $Cu_{5.4}O$-ADSCs group ($P < 0.001$) (Figure 6B). This indicates that $Cu_{5.4}O$-USNPs enhance the angiogenic potential of ADSCs.

Further, immunohistochemical staining for the inflammatory-related factors IL-10 and TNF-α was performed on wound tissues on postoperative day 14. The results showed that the positive rate of the anti-inflammatory factor IL-10 in the $Cu_{5.4}O$-ADSCs group was significantly higher than in the other two groups ($P < 0.001$), while the positive rate of the pro-inflammatory factor TNF-α was lower than in the other two groups ($P < 0.001$) (Figure 7A and B). This indicates a milder inflammatory response in the $Cu_{5.4}O$-ADSCs group, suggesting that $Cu_{5.4}O$-USNPs enhance the anti-inflammatory properties of ADSCs.

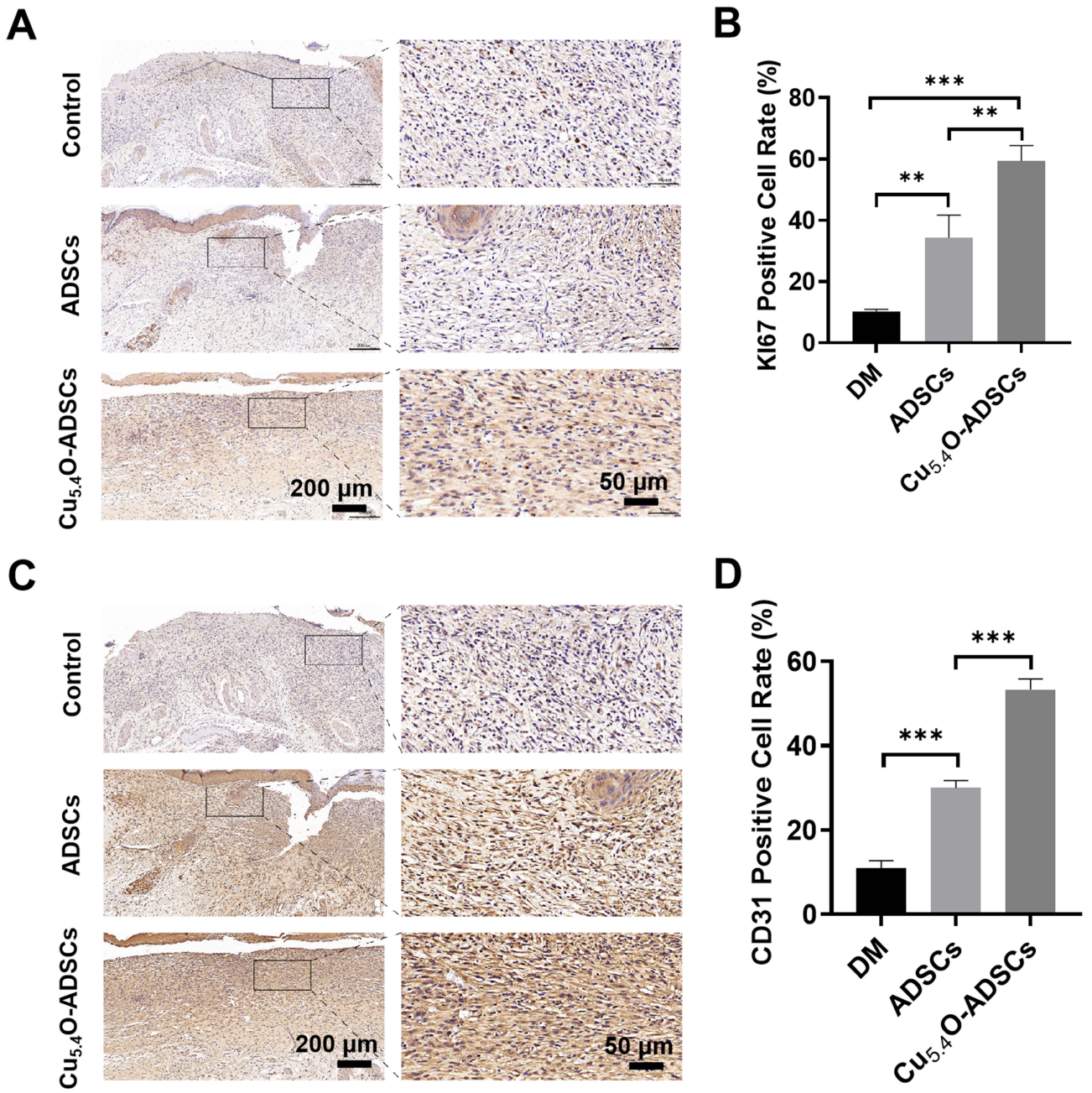

Figure 6 (**A**) Immunohistochemical staining of Ki67 in wound tissues of diabetic mice from different treatment groups on postoperative day 14. (**B**) Quantitative analysis of Ki67 positive expression areas in diabetic mice wounds under different treatment conditions. (**C**) Immunohistochemical staining of CD31 in wound tissues of diabetic mice from different treatment groups on postoperative day 14. (**D**) Quantitative analysis of CD31 positive expression areas in diabetic mice wounds under different treatment conditions. ** $P<0.01$,***$P<0.001$.

Discussion

ADSCs, as adipose-derived mesenchymal stem cells, offer an easier and less painful collection process compared to other stem cell sources, making them a commonly used type of MSCs.[10,49] Despite several studies demonstrating good biocompatibility of $Cu_{5.4}O$-USNPs with various cells, their compatibility with ADSCs remained unreported. Testing revealed that $Cu_{5.4}O$-USNPs exhibit negligible cytotoxicity to ADSCs at working concentrations. Based on these findings, $Cu_{5.4}O$-USNPs were loaded onto ADSCs at safe concentrations and cultured under oxidative stress. Results showed that cell survival rates increased with $Cu_{5.4}O$-USNP concentration, consistent with their concentration-dependent

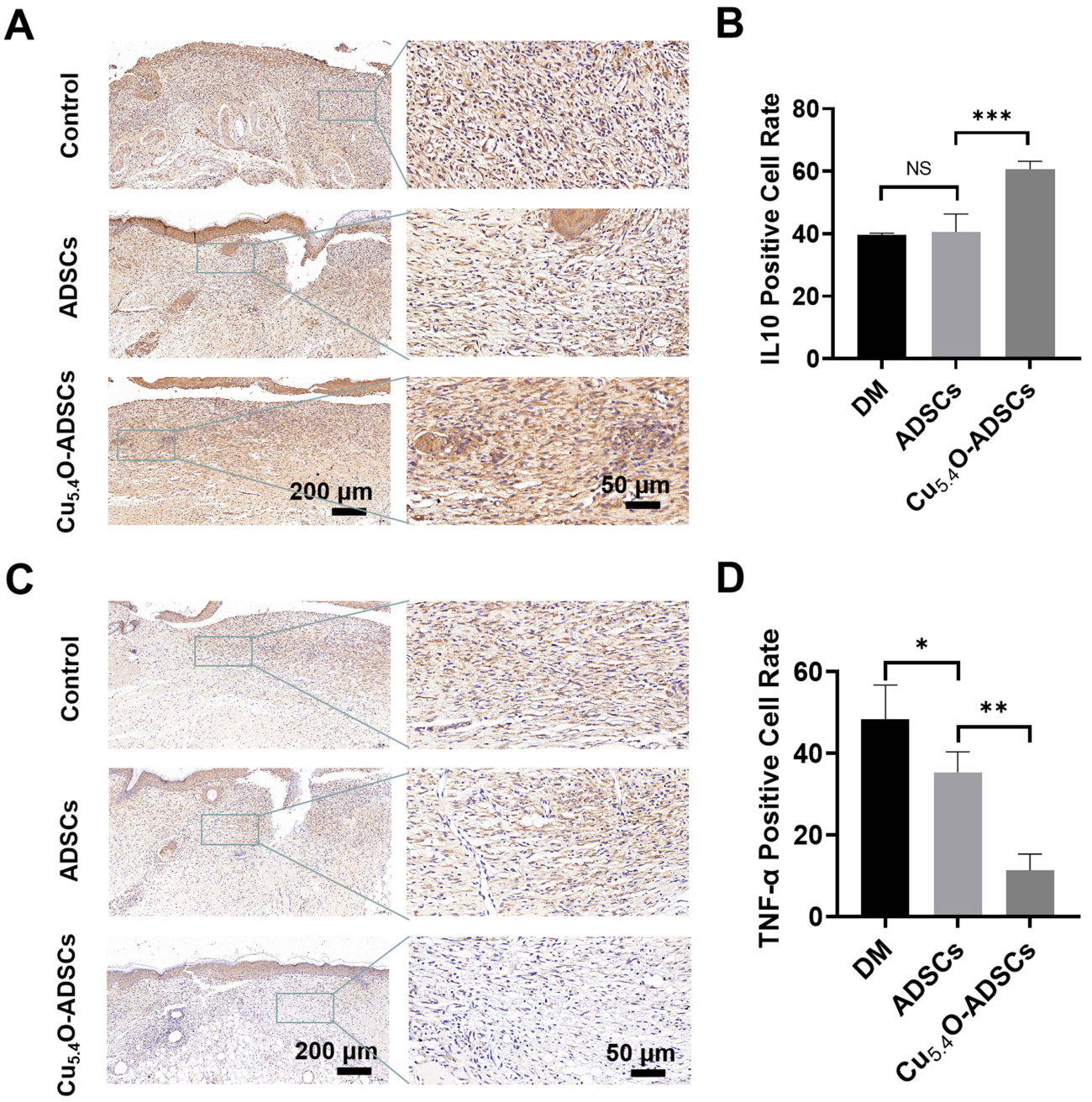

Figure 7 (**A**) Immunohistochemical staining of IL-10 in wound tissues of diabetic mice from different treatment groups on postoperative day 14. (**B**) Quantitative analysis of IL-10 positive expression areas in diabetic mice wounds under different treatment conditions. (**C**) Immunohistochemical staining of TNF-α in wound tissues of diabetic mice from different treatment groups on postoperative day 14. (**D**) Quantitative analysis of TNF-α positive expression areas in diabetic mice wounds under different treatment conditions. *P<0.05,** P<0.01,***P<0.001, NS P>0.05.

antioxidant capacity. Even at 1000 ng/mL, ADSCs maintained high survival rates, comparable to those under normal conditions, indicating efficient ROS elimination by $Cu_{5.4}O$-USNPs in a concentration-dependent manner.

During the wound healing process, antioxidant capacity, paracrine function, and anti-inflammatory capacity each play a crucial role. Antioxidant capacity refers to the ability of an organism to resist damage caused by ROS. During wound healing, ROS levels often increase, leading to oxidative stress that can damage cells and tissues, thereby delaying the healing process. Effective antioxidant capacity can mitigate this damage by neutralizing ROS, thus promoting healing. Paracrine function is the ability of cells to interact with neighboring cells through the secretion of growth factors, cytokines, and other signaling molecules. This function is essential for tissue repair and regeneration. During wound healing, the paracrine factors

released by stem cells can promote the proliferation, migration, and differentiation of local cells, accelerating tissue regeneration. Inflammation is an initial response in the wound healing process. Moderate inflammation helps to clear pathogens and damaged tissues, but excessive inflammation can lead to tissue damage and delayed healing. Enhancing anti-inflammatory capacity helps regulate the inflammatory response and suppress excessive inflammation, facilitating healing. Therefore, enhancing these capacities to effectively promote the use of stem cells in wound repair and improve healing outcomes is a central focus of this study. To further explore the impact of $Cu_{5.4}O$-USNPs on cell activity and function under oxidative stress, antioxidant capacity, paracrine function, and anti-inflammatory ability of ADSCs and $Cu_{5.4}O$-ADSCs were compared. Both the scratch assay and ELISA results demonstrated that $Cu_{5.4}O$-ADSCs maintained cell activity and paracrine function similar to those under normal conditions, even in oxidative stress environments. This suggests that $Cu_{5.4}O$-USNPs provide effective ROS-scavenging, reducing cellular damage and allowing cells to maintain normal functions. An in vitro inflammatory environment was simulated using RAW264.7 cells and LPS, a major component of Gram-negative bacterial cell walls that activates macrophages and induces pro-inflammatory differentiation. This model allowed for the evaluation of anti-inflammatory abilities of ADSCs and $Cu_{5.4}O$-ADSCs. Measurement of pro-inflammatory and anti-inflammatory factors indicated that $Cu_{5.4}O$-ADSCs exhibited stronger anti-inflammatory capabilities in the inflammatory environment. In both oxidative stress and inflammatory conditions, excess ROS production damages cell structures and organelles, triggering apoptosis, autophagy, or necrosis. $Cu_{5.4}O$-USNPs effectively reduce intracellular ROS levels, ensuring cell viability in harmful environments. This enables cells to perform multidirectional differentiation, paracrine signaling, and immune regulation, thereby enhancing their therapeutic effects.

In the diabetic mouse wound model, the impact of $Cu_{5.4}O$-USNPs on ADSCs in promoting wound healing was further investigated. Results indicated that wounds treated with normal ADSCs exhibited a better healing trend compared to PBS-treated wounds, though the difference was not statistically significant. This may be due to ADSCs being affected by the inflammatory environment and continuous ROS generation after transplantation, leading to suppressed cell activity and reduced therapeutic efficacy. In contrast, diabetic wounds treated with $Cu_{5.4}O$-USNP-loaded ADSCs showed significantly improved healing rates compared to those treated with normal ADSCs. Enhanced collagen deposition, increased cell proliferation, and blood vessel formation, along with reduced inflammatory cell infiltration, were observed. This suggests that $Cu_{5.4}O$-USNPs effectively cleared ROS, mitigating the adverse effects of oxidative stress and inflammation on ADSCs, Based on our previous findings and relevant research advancements, we hypothesize that Cu5.4O-USNPs may enhance cellular antioxidant capacity by modulating the Nrf2/ARE signaling pathway, or alleviate inflammation by inhibiting the NF-κB signaling pathway. These effects may help restore normal cellular function and promote diabetic wound healing[46,50–56.] The results from manufacturing, characterization, functionality, and in vitro and in vivo experiments demonstrate that $Cu_{5.4}O$-USNPs significantly enhance the therapeutic potential of ADSCs for treating diabetic wounds. However, several limitations of this study must be acknowledged. First, further tracing detection of $Cu_{5.4}O$-USNPs-loaded ADSCs in cellular experiments was not conducted. Additionally, the study focused on the impact of $Cu_{5.4}O$-USNPs on cell activity, paracrine function, and anti-inflammatory ability of ADSCs without investigating changes in the expression levels of classic pluripotency genes such as CXCR4, Nanog, Oct4, and Sox2, or the multi-lineage differentiation ability of $Cu_{5.4}O$-ADSCs in osteogenesis, adipogenesis, and chondrogenesis. In animal experiments, tracing ADSCs after transplantation into the body remains a challenge that needs to be addressed. Future research should measure biological fluorescence signals to monitor the status of ADSCs at the wound site and conduct a comprehensive assessment of the in vivo biosafety of $Cu_{5.4}O$-USNPs. Addressing these issues will be essential in further improving the therapeutic application of $Cu_{5.4}O$-USNPs-loaded ADSCs.

Conclusions

Overall, the therapeutic effects of ADSCs were enhanced by introducing $Cu_{5.4}O$-USNPs, a biocompatible and highly efficient ROS-clearing nanomaterial. This study demonstrates that $Cu_{5.4}O$-USNPs significantly enhance the antioxidant capacity of ADSCs in diabetic wound healing by scavenging ROS, thereby improving cell activity, paracrine function, and anti-inflammatory ability. The results indicate that ADSCs loaded with $Cu_{5.4}O$-USNPs better promote tissue growth, collagen deposition, cell proliferation, and blood vessel formation, while simultaneously reducing local inflammation,

thus facilitating the healing of diabetic mouse wounds. This nanomaterial shows great promise for enhancing the clinical potential of stem cell therapy and improving the quality of healing for chronic wounds.

Ethical Statement

All animal experimentations were approved by the Institutional Animal Care and Ethics Committee of the affiliated Nanhua hospital, University of South China (Approval ID: 2022-ky-165) and performed in accordance with the principles and procedures of the National Institutes of Health (NIH) Guide for the Care and Use of Laboratory Animals and the Guidelines for Animal Treatment of University of South China.

Acknowledgments

This work was supported by the National Key Clinical Specialty Major Scientific Research Project (No. Z2023083), Hunan Clinical Research Center of Wound Repair and Functional Reconstruction for Hand and Foot (No. 2021SK4030), Hengyang Science and Technology Innovation Plan (No. 202330046272), Fund Project of Hengyang guiding Plan (NO. 202121034573, NO. 202222035846). We thank Bullet Edits Limited for the linguistic editing and proofreading of the manuscript.

Disclosure

The authors declare no conflict of interest.

References

1. Driskill JH, Pan D. Control of stem cell renewal and fate by YAP and TAZ. *Nat Rev Mol Cell Biol*. 2023;24(12):895–911. doi:10.1038/s41580-023-00644-5
2. Ding J-Y, Chen M-J, Wu L-F, et al. Mesenchymal stem cell-derived extracellular vesicles in skin wound healing: roles, opportunities and challenges. *Military Med Res*. 2023;10(1):36. doi:10.1186/s40779-023-00472-w
3. Andrzejewska A, Dabrowska S, Lukomska B, Janowski M. Mesenchymal stem cells for neurological disorders. *Adv Sci*. 2021;8(7):2002944. doi:10.1002/advs.202002944
4. Menasché P. Mesenchymal stromal cell therapy for heart failure: never stop dreaming. *J Am Coll Cardiol*. 2023;81(9):864–866. doi:10.1016/j.jacc.2022.12.019
5. Lu B, Lerman LO. MSC therapy for diabetic kidney disease and nephrotic syndrome. *Nat Rev Nephrol*. 2023;19(12):754–755. doi:10.1038/s41581-023-00776-z
6. Kadri N, Amu S, Iacobaeus E, Boberg E, Le Blanc K. Current perspectives on mesenchymal stromal cell therapy for graft versus host disease. *Cell Mol Immunol*. 2023;20(6):613–625. doi:10.1038/s41423-023-01022-z
7. Yan W, Chen Y, Guo Y, et al. Irisin promotes cardiac homing of intravenously delivered MSCs and protects against ischemic heart injury. *Adv Sci*. 2022;9(7):e2103697. doi:10.1002/advs.202103697
8. Frenz-Wiessner S, Klein C. Using stem cells to model the human bone marrow in a dish. *Nat Methods*. 2024;21(5):762–763. doi:10.1038/s41592-024-02173-1
9. Han Y, Yang J, Fang J, et al. The secretion profile of mesenchymal stem cells and potential applications in treating human diseases. *Signal Transduct Target Ther*. 2022;7(1):92. doi:10.1038/s41392-022-00932-0
10. Smirnova A, Yatsenko E, Baranovskii D, Klabukov I. Mesenchymal stem cell-derived extracellular vesicles in skin wound healing: the risk of senescent drift induction in secretome-based therapeutics. *Military Med Res*. 2023;10(1):60. doi:10.1186/s40779-023-00498-0
11. Fan XL, Zhang Y, Li X, Fu QL. Mechanisms underlying the protective effects of mesenchymal stem cell-based therapy. *Cell Mol Life Sci*. 2020;77(14):2771–2794. doi:10.1007/s00018-020-03454-6
12. Zakrzewski W, Dobrzyński M, Szymonowicz M, Rybak Z. Stem cells: past, present, and future. *Stem Cell Res Ther*. 2019;10(1):68. doi:10.1186/s13287-019-1165-5
13. Uccelli A, Moretta L, Pistoia V. Mesenchymal stem cells in health and disease. *Nat Rev Immunol*. 2008;8(9):726–736. doi:10.1038/nri2395
14. Srinivas US, Tan BWQ, Vellayappan BA, Jeyasekharan AD. ROS and the DNA damage response in cancer. *Redox Biol*. 2019;25:101084. doi:10.1016/j.redox.2018.101084
15. Ye X, Xia L, Yang H, et al. Reactive oxygen/nitrogen species scavenging multi-enzyme mimetic ultrasmall calcium hexacyanoferrate (III) nanozyme for hypertension remedy. *Mater Today*. 2023;68:148–163. doi:10.1016/j.mattod.2023.06.015
16. Zhang J, Wang X, Vikash V, et al. ROS and ROS-mediated cellular signaling. *Oxid Med Cell Longev*. 2016;2016:4350965. doi:10.1155/2016/4350965
17. Sies H, Jones DP. Reactive oxygen species (ROS) as pleiotropic physiological signalling agents. *Nat Rev Mol Cell Biol*. 2020;21(7):363–383. doi:10.1038/s41580-020-0230-3
18. Young IS, Woodside JV. Antioxidants in health and disease. *J Clin Pathol*. 2001;54(3):176–186. doi:10.1136/jcp.54.3.176
19. Liu J, Han X, Zhang T, Tian K, Li Z, Luo F. Reactive oxygen species (ROS) scavenging biomaterials for anti-inflammatory diseases: from mechanism to therapy. *J Hematol Oncol*. 2023;16(1):116. doi:10.1186/s13045-023-01512-7
20. Sosa V, Moliné T, Somoza R, Paciucci R, Kondoh H, L MEL. Oxidative stress and cancer: an overview. *Ageing Res Rev*. 2013;12(1):376–390. doi:10.1016/j.arr.2012.10.004

21. Parikh K, Warren C, Caracio R. Education on reactive oxygen species to lay the foundation for understanding therapeutic advances in anticancer therapy. *J Clin Oncol*. 2021;39(3_suppl):478. doi:10.1200/JCO.2021.39.3_suppl.478
22. van der Pol A, van Gilst WH, Voors AA, van der Meer P. Treating oxidative stress in heart failure: past, present and future. *Eur J Heart Fail*. 2019;21(4):425–435. doi:10.1002/ejhf.1320
23. Lee CY, Wu SW, Yang JJ, et al. Vascular endothelial dysfunction induced by 3-bromofluoranthene via MAPK-mediated-NFκB pro-inflammatory pathway and intracellular ROS generation. *Arch Toxicol*. 2024;98(7):2247–2259. doi:10.1007/s00204-024-03751-0
24. Islam MT. Oxidative stress and mitochondrial dysfunction-linked neurodegenerative disorders. *Neurol Res*. 2017;39(1):73–82. doi:10.1080/01616412.2016.1251711
25. Tönnies E, Trushina E. Oxidative stress, synaptic dysfunction, and alzheimer's disease. *J Alzheimers Dis*. 2017;57(4):1105–1121. doi:10.3233/jad-161088
26. Cheng F, Kotha S, Fu M, et al. Nanozyme enabled protective therapy for neurological diseases. *Nano Today*. 2024;54:102142. doi:10.1016/j.nantod.2023.102142
27. He M, Zhang X, Ran X, et al. Black phosphorus nanosheets protect neurons by degrading aggregative α-syn and clearing ROS in parkinson's disease. *Adv Mater*. 2024;36:e2404576. doi:10.1002/adma.202404576
28. Dunnill C, Patton T, Brennan J, et al. Reactive oxygen species (ROS) and wound healing: the functional role of ROS and emerging ROS-modulating technologies for augmentation of the healing process. *Int Wound J*. 2017;14(1):89–96. doi:10.1111/iwj.12557
29. Chen Y, Yang X, Li K, et al. Phenolic ligand–metal charge transfer induced copper nanozyme with reactive oxygen species-scavenging ability for chronic wound healing. *ACS Nano*. 2024;18(9):7024–7036. doi:10.1021/acsnano.3c10376
30. Yang S, Sun Y, Yan C. Recent advances in the use of extracellular vesicles from adipose-derived stem cells for regenerative medical therapeutics. *J Nanobiotechnology*. 2024;22(1):316. doi:10.1186/s12951-024-02603-4
31. Wan X, Ni X, Xie Y, et al. Research progress and application prospect of adipose-derived stem cell secretome in diabetes foot ulcers healing. *Stem Cell Res Ther*. 2024;15(1):279. doi:10.1186/s13287-024-03912-z
32. Hao Z, Qi W, Sun J, Zhou M, Guo N. Review: research progress of adipose-derived stem cells in the treatment of chronic wounds. *Front Chem*. 2023;11:1094693. doi:10.3389/fchem.2023.1094693
33. Yan D, Song Y, Zhang B, et al. PMID: 38167106. Progress and application of adipose-derived stem cells in the treatment of diabetes and its complications. *Stem Cell Res Ther*. 2024;15(1):3. doi:10.1186/s13287-023-03620-0
34. Mendez JJ, Ghaedi M, Sivarapatna A, et al. Mesenchymal stromal cells form vascular tubes when placed in fibrin sealant and accelerate wound healing in vivo. *Biomaterials*. 2015;40:61–71. doi:10.1016/j.biomaterials.2014.11.011
35. Ko E, Lee KY, Hwang DS. Human umbilical cord blood-derived mesenchymal stem cells undergo cellular senescence in response to oxidative stress. *Stem Cells Dev*. 2012;21(11):1877–1886. doi:10.1089/scd.2011.0284
36. Orciani M, Gorbi S, Benedetti M, et al. Oxidative stress defense in human-skin-derived mesenchymal stem cells versus human keratinocytes: different mechanisms of protection and cell selection. *Free Radic Biol Med*. 2010;49(5):830–838. doi:10.1016/j.freeradbiomed.2010.06.007
37. He Z, Sun C, Ma Y, et al. Rejuvenating aged bone repair through multihierarchy reactive oxygen species-regulated hydrogel. *Adv Mater*. 2024;36(9):e2306552. doi:10.1002/adma.202306552
38. Denu RA, Hematti P. Effects of oxidative stress on mesenchymal stem cell biology. *Oxid Med Cell Longev*. 2016;2016:2989076. doi:10.1155/2016/2989076
39. Yang B, Chen Y, Shi J. Reactive oxygen species (ROS)-based nanomedicine. *Chem Rev*. 2019;119(8):4881–4985. doi:10.1021/acs.chemrev.8b00626
40. Li L, Xiao B, Mu J, et al. A MnO(2) nanoparticle-dotted hydrogel promotes spinal cord repair via regulating reactive oxygen species microenvironment and synergizing with mesenchymal stem cells. *ACS Nano*. 2019;13(12):14283–14293. doi:10.1021/acsnano.9b07598
41. Hao T, Li J, Yao F, et al. Injectable fullerenol/alginate hydrogel for suppression of oxidative stress damage in brown adipose-derived stem cells and cardiac repair. *ACS Nano*. 2017;11(6):5474–5488. doi:10.1021/acsnano.7b00221
42. Li J, Zhang J, Chen Y, Kawazoe N, Chen G. TEMPO-conjugated gold nanoparticles for reactive oxygen species scavenging and regulation of stem cell differentiation. *ACS Appl Mater Interfaces*. 2017;9(41):35683–35692. doi:10.1021/acsami.7b12486
43. Shen H, Cheng L, Zheng Q, Liu W, Wang Y. Scavenging of reactive oxygen species can adjust the differentiation of tendon stem cells and progenitor cells and prevent ectopic calcification in tendinopathy. *Acta Biomater*. 2022;152:440–452. doi:10.1016/j.actbio.2022.09.007
44. Tang C, Luo J, Yan X, et al. Melanin nanoparticles enhance the neuroprotection of mesenchymal stem cells against hypoxic-ischemic injury by inhibiting apoptosis and upregulating antioxidant defense. *Cell Biol Int*. 2022;46(6):933–946. doi:10.1002/cbin.11781
45. Arai Y, Park H, Park S, et al. Bile acid-based dual-functional prodrug nanoparticles for bone regeneration through hydrogen peroxide scavenging and osteogenic differentiation of mesenchymal stem cells. *J Control Release*. 2020;328:596–607. doi:10.1016/j.jconrel.2020.09.023
46. Liu T, Xiao B, Xiang F, et al. Ultrasmall copper-based nanoparticles for reactive oxygen species scavenging and alleviation of inflammation related diseases. *Nat Commun*. 2020;11(1):2788. doi:10.1038/s41467-020-16544-7
47. Peng Y, He D, Ge X, et al.. Construction of heparin-based hydrogel incorporated with Cu5.4O ultrasmall nanozymes for wound healing and inflammation inhibition. *Bioact Mater*. 2021;6(10):3109–3124. Erratum in: Bioact Mater. 2024 Jun 14;40:275-279. doi: 10.1016/j.bioactmat.2024.06.006. doi:10.1016/j.bioactmat.2021.02.006
48. Facchin BM, Dos Reis GO, Vieira GN, et al. Inflammatory biomarkers on an LPS-induced RAW 264.7 cell model: a systematic review and meta-analysis. Inflamm Res. 2022;71(7–8):741–758. doi:10.1007/s00011-022-01584-0
49. Mazini L, Rochette L, Admou B, Amal S, Malka G. Hopes and limits of adipose-derived stem cells (ADSCs) and mesenchymal stem cells (MSCs) in wound healing. *Int J Mol Sci*. 2020;21(4):1306. doi:10.3390/ijms21041306
50. Li J, Wang D, Liu Y, Zhou Y. Role of NRF2 in colorectal cancer prevention and treatment. *Technol Cancer Res Treat*. 2022;21:15330338221105736. doi:10.1177/15330338221105736
51. Zhou YF, Liu HW, Yang X, Li CX, Chen JS, Chen ZP. Probucol attenuates high glucose-induced Müller cell damage through enhancing the Nrf2/p62 signaling pathway. *Int Ophthalmol*. 2023;43(12):4595–4604. doi:10.1007/s10792-023-02859-z
52. Lin L, Wu Q, Lu F, et al. Nrf2 signaling pathway: current status and potential therapeutic targetable role in human cancers. *Front Oncol*. 2023;13:1184079. doi:10.3389/fonc.2023.1184079

53. Chen Z, Jin M, He H, et al. Mesenchymal stem cells and macrophages and their interactions in tendon-bone healing. *J Orthop Translat*. 2023;39:63–73. doi:10.1016/j.jot.2022.12.005
54. Long T, Li C, Xu F, Xiao J. Therapeutic efficacy of platelet-rich fibrin on surgical site wound healing in patients undergoing oral carcinoma resection: a meta-analysis. *Int Wound J*. 2024;21(1):e14386. doi:10.1111/iwj.14386
55. Qin W, Liu K, Su H, et al. Tibial cortex transverse transport promotes ischemic diabetic foot ulcer healing via enhanced angiogenesis and inflammation modulation in a novel rat model. *Eur J Med Res*. 2024;29(1):155. doi:10.1186/s40001-024-01752-4
56. Wu NH, Ke ZQ, Wu S, et al. Evaluation of the antioxidant and endothelial protective effects of Lysimachia christinae Hance (Jin Qian Cao) extract fractions. *BMC Complement Altern Med*. 2018;18(1):128. doi:10.1186/s12906-018-2157-1